A scaffold protein that chaperones a cysteine-sulfenic acid in H2O2 signaling

Antoine Bersweiler, Benoît d'Autréaux, Hortense Mazon, Alexandre Kriznik, Gemma Belli, Agnès Delaunay-Moisan, Michel B Toledano, Sophie Rahuel-Clermont

Title

A scaffold protein that chaperones a cysteine-sulfenic acid in H_2O_2 signaling

by

Antoine Bersweiler[1], Benoît d'Autréaux[2], Hortense Mazon[1], Alexandre Kriznik[1], Gemma Belli[2,3], Agnès Delaunay-Moisan[2], Michel B Toledano[2]* & Sophie Rahuel-Clermont[1]*

[1] UMR 7365 CNRS-Université de Lorraine IMoPA, Biopôle, campus Biologie-Santé, 9 avenue de la Forêt de Haye, BP 20199, F-54505 Vandœuvre-lès-Nancy Cédex, France

[2] Institute for Integrative Biology of the Cell (I2BC), UMR9198, CNRS, CEA-Saclay, Université Paris-Saclay, iBiTecS/SBIGEM, Laboratoire Stress oxydant et Cancer, Bat 142, F-91198 Gif-sur-Yvette Cedex, France

[3] present address: Department of Basic Medical Sciences, IRB Lleida, University of Lleida, Lleida 25198 Spain

* Corresponding authors

e-mail: sophie.rahuel@univ-lorraine.fr, tel., +33 372 746 660

e-mail: michel.toledano@cea.fr, tel., +33 169 088 244

ABSTRACT

In *Saccharomyces cerevisiae,* Yap1 regulates an H_2O_2-inducible transcriptional response that controls cellular H_2O_2 homeostasis. H_2O_2 activates Yap1 by oxidation through the intermediacy of the thiol-peroxidase Orp1. Upon reacting with H_2O_2, Orp1 catalytic cysteine oxidizes to a sulfenic acid, which then engages either into an intermolecular disulfide with Yap1 that leads to Yap1 activation, or an intramolecular disulfide that commits the enzyme into its peroxidatic cycle. Of these two competing reactions, how the former one, which is kinetically unfavorable, occurs? We show that the Yap1-binding-protein Ybp1 brings together Orp1 and Yap1 into a ternary complex that selectively activates condensation of the Orp1 sulfenylated cysteine with one of the six Yap1 cysteines, while inhibiting Orp1 intramolecular disulfide formation. We propose that Ybp1 operates as a scaffold protein and as a sulfenic acid chaperone to provide specificity into the transfer of oxidizing equivalents by a reactive sulfenic acid species.

Reactive oxygen species (ROS), which include the superoxide anion ($O_2^{\bullet -}$) and hydrogen peroxide (H_2O_2), are toxic molecules that also operate in intracellular signaling. Both these effects are due to ROS chemical reactivity, which enables them to oxidize biological molecules, thereby causing either damage, or modifying the activity of regulatory proteins by covalent modification. Whereas the toxicity of ROS is intuitively perceived, their signaling function has been more difficult to grasp, owing to the paradox posed by the specificity required for signaling and the seeming indiscriminate reactivity of ROS[1].

ROS-responsive pathways that regulate ROS intracellular homeostasis in microorganisms have provided, and still are, fundamental principles of how specificity can be achieved in ROS signaling[1]. These pathways make use of sensors that "measure" the intracellular concentration of ROS and proportionally set the expression of antioxidants, thereby maintaining ROS concentration below a toxic threshold[2]. One such pathway is the *S. cerevisiae* H_2O_2-responsive transcription factor Yap1, which activates most antioxidants, thiol-reductases, and other stress defense and detoxifying activities[2]. Yap1 is primarily controlled at the level of nucleo-cytoplasmic shuttling[3]. H_2O_2 oxidizes Yap1 into two disulfides between Cys residues C303-C598 and C310-C629[4–6] (**Supplementary results, Supplementary Fig. 1**). The conformation change resulting from this oxidation conceals a nuclear export signal, which by inhibiting nuclear export promotes Yap1 accumulation into the nucleus[4,7,8].

Yap1 oxidation by H_2O_2 is mediated by the thiol-based Oxidant Receptor and Peroxidase Orp1[9] (**Fig. 1)**. Reaction of Orp1 catalytic Cys residue (C36) with H_2O_2 yields a sulfenic acid (Orp1—SOH) (reaction 1)[10,11]. Once formed, the C36-SOH can engage into either an intermolecular disulfide with Yap1 by condensation with Yap1 C598 yielding Orp1—S—S—Yap1 (reaction 2), which is then transposed into the first intramolecular disulfide of active Yap1, or into an Orp1 intramolecular disulfide by condensation with Orp1 resolving Cys residue (C82) ($Orp1_{OxSS}$, reaction 3), which commits the enzyme into its peroxidatic cycle[9]. Of these two competing reactions, the unimolecular

62 one that produces $Orp1_{OxSS}$ should be kinetically favored over the bimolecular one[12] engaging Orp1
63 and Yap1, which raises the question of the mechanism that enable the latter to occur. The Yap1-
64 binding protein Ybp1 is required for the Orp1-dependent oxidation of Yap1 by H_2O_2[13–15]. As it co-
65 precipitates with Yap1, Ybp1 could favor the Orp1/Yap1 redox interaction by bringing these
66 proteins together, and could also guide Orp1—SOH towards Yap1 C598, or prevent formation of the
67 competing Orp1 C36-C82 disulfide[2].

68 We sought elucidating Ybp1 function by measuring the kinetics of Orp1-dependent oxidation
69 of Yap1 by H_2O_2 upon reconstitution of the redox relay *in vitro*, and by probing the interactions
70 between the redox relay partners. We found that Ybp1 brings together Orp1 and Yap1 into a ternary
71 complex, in which Orp1—S—S—Yap1 intermolecular disulfide formation is activated, while
72 $Orp1_{OxSS}$ intramolecular disulfide formation is impeded, hence favoring H_2O_2 signaling at the
73 expense of H_2O_2 scavenging. Our data suggest a novel mechanism whereby by shielding and
74 canalizing the reactivity of the Cys-sulfenic acid, Ybp1 operate as a "sulfenic acid chaperone", an
75 issue important in view of the emerging roles of thiol peroxidases[16,17] and sulfenic acid species[17–19]
76 in redox biology.

RESULTS

Ybp1 brings Yap1 and Orp1 in a non-covalent 1:1:1 complex

We first assayed the interaction of Ybp1 and Yap1 *in vitro*. When alone in solution, Ybp1 eluted from a size-exclusion column as a single peak with an apparent mass of 100 kDa, close to the calculated monomer mass (80 kDa), and Yap1 as a major peak of 470 kDa (calculated monomer mass = 73 kDa), which suggested that Yap1 oligomerizes in solution and/or adopts a non-globular, flexible conformation, in accordance with its sensitivity to proteolysis[5] (**Fig. 2a**). A small fraction of Yap1 also eluted within the column-void volume, likely reflecting protein aggregation. When present in an equimolar mix, the two proteins now eluted as one major species with an apparent mass of 307 kDa, confirming the Ybp1-Yap1 interaction shown by co-immunoprecipitation from crude lysates[13,14] and suggesting the presence of a 1:1 complex (calculated mass of 153 kDa) with a non-globular conformation, or a 2:2 complex (306 kDa). Doubling the concentration of Yap1 relative to Ybp1 produced an additional peak corresponding to free Yap1, thus confirming non-covalent complex formation with a stoichiometry of 1:1 or 2:2 (hereafter referred to as Ybp1·Yap1). Quantitative data of the Yap1-Ybp1 interaction were obtained from the change of fluorescence anisotropy of fluorochrome-labeled Ybp1 (AF-Ybp1) upon Yap1 titration. A saturable 11% anisotropy increase was observed, which after conversion to the fraction of bound AF-Ybp1, was fitted to a single-site binding equation, yielding a dissociation constant of 1.6 ± 0.3 µM (**Fig. 2b**). Using Yap1$^{SSS\ SSS}$, a mutant with Ser substitution of all six Cys, gave a value close to the previous one (0.7 ± 0.2 µM). Titration of labeled Yap1 (AF-Yap1) by Ybp1 produced a saturable 22% fluorescence anisotropy increase and a dissociation constant of 1.3 ± 0.2 µM, very close to the value obtained using AF-Ybp1.

We next assayed the interaction of Orp1 with its two partners by isothermal titration calorimetry (ITC). Yap1$^{SSS\ SSS}$ was used here to avoid any redox interferences. No significant signal was observed when Orp1 was injected into a Yap1$^{SSS\ SSS}$ solution (**Fig. 2c**, left panel). In contrast, injection of Orp1 into a Ybp1 solution produced a binding isotherm that fitted a single-site model,

which yielded a dissociation constant of 0.8 ± 0.1 μM and a stoichiometry of 0.8 ± 0.1, indicative of a 1:1 stoichiometry (**Fig. 2c**, central panel, **Supplementary Table 1**). Calorimetric titration of the Ybp1·Yap1 complex by Orp1 also produced an isotherm corresponding to a single-site binding interaction with a dissociation constant of 0.7 ± 0.2 μM and a stoichiometry of 0.8 ± 0.1 (**Fig. 2c,** right panel**, Supplementary Table 1**), also indicative of a 1:1 stoichiometry, which indirectly confirmed a Ybp1-Yap1 1:1 association. In the latter experiment, Orp1 binding to Ybp1 could have dissociated the Ybp1·Yap1 complex, but predicted titrations that incorporated the Ybp1·Yap1 and Orp1·Ybp1 dissociation constants did not reach complete saturation under the conditions used. No significant signal was detected by titrating Ybp1 or the Ybp1·Yap1$^{SSS\ SSS}$ complex with Orp1 in the intramolecular disulfide form $Orp1_{OxSS}$ (**Supplementary Fig. 2**). TAP-Tag-affinity precipitation of Ybp1 from crude yeast lysates brought down both Yap1 and Orp1, thus establishing that the ternary Orp1·Ybp1·Yap1 complex is also formed *in vivo*, although we cannot totally rule out that Orp1 coprecipitates with Ybp1 by virtue of its disulfide linkage to Yap1 (**Supplementary Fig. 3**).

Ybp1 thus brings together Yap1 and reduced Orp1, but not $Orp1_{OxSS}$, into a non-covalent ternary Orp1·Ybp1·Yap1 complex of 1:1:1 stoichiometry.

In vitro reconstitution of the Orp1-Yap1 redox relay

To address the molecular function of Ybp1, we reconstituted the redox relay *in vitro* with purified Yap1, Orp1, Ybp1, thioredoxin (Trx), Trx reductase and NADPH, and monitored the kinetics of Yap1 oxidation by H_2O_2 by the differential migration of Yap1 redox conformers by non-reducing SDS-PAGE. As previously shown[9], Myc-Yap1 from untreated cells migrates as a unique band ($Yap1_{red}$); minutes after H_2O_2 exposure, the C36-C598-linked Orp1—S—S—Yap1 complex and Yap1 intramolecular disulfide forms ($Yap1_{ox}$) are both seen as two distinct bands that migrate above and below reduced Yap1, respectively (**Fig. 3a, Supplementary Fig. 4**). A third H_2O_2-inducible Myc-immunoreactive band was also seen just above Orp1—S—S—Yap1, which also contains Orp1 and possibly leads to formation of the second Yap1 intramolecular disulfide. Analysis of the

129 reconstituted relay similarly identified reduced Yap1 and Ybp1 prior to addition of H_2O_2, and then
130 three new Yap1 electrophoretic forms upon addition of H_2O_2, which correspond to the Yap1-
131 intramolecular disulfide forms and to the two Orp1-Yap1 disulfide-linked complexes (**Fig. 3b)**. Yap1
132 oxidation was fast, occurring within seconds, and lasted a few minutes after which Yap1 returned to
133 its reduced form, closely reproducing the *in vivo* kinetics of Yap1 oxidation[9].
134
135 **Orp1 and Ybp1 are required for Yap1 oxidation *in vitro***
136 We next probed each of the components of the redox relay on Yap1 oxidation. When alone,
137 Yap1 (5 μM) became oxidized, but at very high doses of H_2O_2, much higher than those effective in
138 the fully reconstituted system (H_2O_2 > 500 μM *vs* < 100 μM), with appearance of Yap1 high
139 molecular weight disulfide-linked complexes, indicative of non-native disulfide bond formation
140 (**Supplementary Fig. 5a**). Excluding the Trx system from the reaction did not alter Yap1 oxidation,
141 except for a slower kinetics, likely due to the trapping of Orp1 in the $Orp1_{OxSS}$ form (**Supplementary**
142 **Fig. 5b**). Excluding Orp1 however prevented Yap1 oxidation by H_2O_2 at 100 μM (**Supplementary**
143 **Fig. 5c**), thus confirming Orp1 absolute requirement for Yap1 oxidation[9,13]. Similarly, excluding
144 Ybp1 prevented Yap1 oxidation by H_2O_2 at 100 μM (**Supplementary Fig. 5b**). Only at a very high
145 dose of H_2O_2 (2 mM), a slow and weak oxidation of Yap1 was observed (**Fig. 3c**), which was partially
146 dependent upon Orp1 (10 μM), as indicated the presence of a very weak band corresponding to the
147 Orp1-Yap1 disulfide complex. Introducing Ybp1 led to a concentration-dependent stimulation of
148 Yap1 oxidation, and appearance of one, and then of the two Orp1-Yap1 disulfide-linked complexes
149 (**Fig. 3c**). The effect of Ybp1 reached a maximum at a Ybp1:Yap1 ratio of 1:1, thus confirming the
150 results of **Fig. 2**.
151
152 **Ybp1 is required for the formation of Orp1—S—S—Yap1**
153 As previously observed *in vivo* (**Fig. 3a**), Ala substitution of Yap1 C303 ($Yap1^{C303A}$) stabilizes
154 the Orp1-Yap1 C36-C598 intermolecular disulfide by preventing its transposition into the C303-

C598 intramolecular Yap1 disulfide[9]. In Δ*ybp1* cells that expressed Yap1^{C303A} however, the Orp1—S—S—Yap1 complex did not form (**Fig. 3a**). Similarly, in the reconstituted system, Yap1^{C303A} formed a stable Orp1—S—S—Yap1 complex with Orp1 in the presence, but not in the absence of Ybp1 (**Fig. 3d**). The peroxiredoxin Tsa1 was proposed to replace Orp1 in Yap1 oxidation in cells lacking Ybp1[20], but no band corresponding to a Tsa1-Yap1 adduct was detected in Δ*ybp1*, as also reported[20].

The reconstituted system thus faithfully reproduces the *in vivo* setting, thereby confirming the requirement of both Orp1 and Ybp1 for efficient and sensitive Yap1 oxidation by H_2O_2. Furthermore, both *in vivo* and *in vitro* data indicate that Ybp1 is required for the initial Orp1-Yap1 redox interaction (reaction 2, see **Fig. 1**).

Ybp1 activates formation of Orp1—S—S—Yap1

The Orp1-Yap1 redox relay can be deconstructed into three single reactions: formation of the Orp1—SOH (reaction 1, rate constant k_{SOH}); condensation of the former with Yap1 C598 (reaction 2) or with Orp1 C82 (reaction 3, rate constant k_{SS}) (see **Fig. 1**). To test whether Ybp1 modulates reactions 2, or 3 or both, we assessed its effect on their kinetics using a quench flow apparatus.

Reaction 2 was evaluated with an Orp1 mutant only retaining C36 (Orp1 C64S, C82A, Orp1^{CSA}) to eliminate reaction 3, and a Yap1 mutant only retaining C598 (Yap1$^{SSS\ CSS}$), to avoid unwanted redox reactions. In the absence of Ybp1, these two mutants engaged in the stable Orp1—S—S—Yap1 disulfide by lack of Yap1 C303 (**Supplementary Fig. 6**, also showing that Orp1^{C82S} behaves as Orp^{CSA}). We also used H_2O_2 at concentrations low enough to avoid non-specific oxidation (100 μM) which would still ensure fast enough Orp1—SOH formation, for the latter not to be rate limiting for the overall reaction (k_{SOH} = 1.6 $10^5 \pm 0.1$ $M^{-1}s^{-1}$, which gives a rate constant of 16 s^{-1} at 100 μM H_2O_2, see **Supplementary Fig. 7**). Reactions were started by mixing H_2O_2 to a mixture containing excess Orp1^{CSA} and either Yap1$^{SSS\ CSS}$ or the Ybp1·Yap1$^{SSS\ CSS}$ complex, and were stopped by acid quenching. Prior to H_2O_2 addition, reverse-phase chromatograms of the reaction mixtures lacking Ybp1 identified Yap1$^{SSS\ CSS}$ (peak 1) and Orp1^{CSA} (peak 4) (**Supplementary Fig. 8** and **Supplementary**

Table 2). Upon H_2O_2 addition, the Yap1 and Orp1^{CSA} peaks gradually decreased over time, and three additional peaks appeared with masses compatible with Orp1—S—S—Yap1 (peak 2), disulfide-linked homodimeric Orp1 (C36—S—S—C36) (peak 5), and oxidized Orp1^{CSA} in the sulfenylamide form (peak 3) (**Supplementary Fig. 8** and **Supplementary Table 2**). The latter species likely forms by Orp1—SOH intramolecular cyclization upon attack of the neighboring Gly37 amide nitrogen at acidic pH[21–23]. Chromatograms of reaction mixtures containing Ybp1 yielded the same products as those observed in its absence (**Fig 4a**).

The kinetics of Orp1—S—S—Yap1 formation in the absence and presence of Ybp1 were deduced from the evolution of peak-2 area, yielding respective observed rate constants of 0.3 ± 0.03 and 2.6 ± 0.4 s^{-1}, which indicated a significant stimulatory effect of Ybp1 (**Fig. 4b**). Reacting H_2O_2 in a mixture containing wild-type (Wt) Orp1 and the Ybp1·Yap1$^{SSS\ CSS}$ complex led again to a decrease of Yap1$^{SSS\ CSS}$ (peak 1) and Orp1 (peak 8), and the appearance of Orp1$_{OxSS}$ (peak 7) and of a species with mass compatible with Orp1—S—S—Yap1 (peak 6) (**Fig. 4c, Supplementary Table 2**). The latter appeared at an observed first-order rate constant of 4.6 ± 0.2 s^{-1} (**Fig. 4d**). This value did not change by increasing Orp1 concentration up to near saturation (10 to 80 µM) (mean 5.6 ± 1.0 s^{-1}), further demonstrating that Orp1 operates within the Orp1·Ybp1·Yap1 ternary complex (**Fig. 4d**, inset), and hence that the reaction should obey saturation kinetics, in contrast to the bimolecular one measured in the absence of Ybp1 (Orp1 and Yap1 do not form a pre-complex).

The kinetics of Orp1—S—S—Yap1 formation in the absence of Ybp1 (**Supplementary Fig. 8**, **Fig. 4b**) was analyzed by directly fitting data to a two-step model, which comprises reaction 1 (k_{SOH} = $1.6\ 10^5 \pm 0.1$ $M^{-1}s^{-1}$, **Supplementary Fig. 7**) followed by reaction 2 (**Supplementary Fig. 9a)**. This analysis yielded a second order rate constant $k_{bimolecular}$ for reaction 2 of $(7.4 \pm 4.9)10^3$ $M^{-1}s^{-1}$. To interpret the kinetics obtained in presence of Ybp1 (**Fig. 4a,b**), we directly fitted data to a similar reaction scheme that was now preceded by the formation of the ternary complex, assumed to be a rapid equilibrium characterized by the K affinity constant between Ybp1·Yap1$^{SSS\ CSS}$ and Orp1 of 0.7 µM (**Supplementary Fig. 9b**). This analysis yielded a first order rate constant for reaction 2 in the

complex $k_{complex}$ of 3.5 ± 0.7 s^{-1}, close to the observed value of 2.6 s^{-1}. We then compared the value of $\frac{k_{complex}}{K}$ (5.0 10^6 $M^{-1}s^{-1}$ for $Orp1^{CSA}$) to the $k_{bimolecular}$ value of 7.4 10^3 $M^{-1}s^{-1}$ obtained in the absence of Ybp1. The 700-fold ratio between these two parameters reveals the actual impact of Ybp1 on reaction 2, which becomes particularly significant when considering the low *in vivo* concentrations of Orp1 and Yap1 (**Supplementary Fig. 9c**). Reacting oxidized Orp1 ($Orp1_{OxSS}$) under the same conditions yielded an observed rate constant of 0.026 ± 0.006 s^{-1}, nearly 200-times slower relative to the reaction with reduced Orp1 (**Fig. 4e,f**).

These data indicate a strong increasing effect of Ybp1 on the rate of reaction of Yap1 C598 with Orp1—SOH, akin to enzyme catalysis, which is accounted for by Ybp1-dependent pre-complex formation and possibly also by a chemical activation of the reaction within the Orp1·Ybp1·Yap1 ternary complex. They also confirm that $Orp1_{OxSS}$ is not competent for Yap1 oxidation.

$Orp1_{OxSS}$ formation is impeded in the ternary complex

We next explored whether Ybp1 could also favor reaction 2 by inhibiting reaction 3. We first evaluated the effect of Ybp1 and Yap1 on Orp1 peroxidase activity, as measured by the rate of NADPH consumption under multiple turnovers, *i.e.* in the presence of Trx and Trx reductase. In the presence of $Yap1^{SSS\ SSS}$ —used here and below to prevent reaction 2— or Ybp1, Orp1 activity was not altered. In contrast, in their presence in equimolar amounts, Orp1 peroxidase activity was strongly inhibited up to 88% and 97%, at 1 and 20 µM of added proteins, respectively (**Supplementary Fig. 10a**). This effect was not due to inhibition of the Trx system since Yap1 and Ybp1 did not alter Trx-dependent recycling of a peroxiredoxin and methionine sulfoxide reductase (**Supplementary Fig 10b**).

Inhibition of the Orp1 peroxidatic cycle might occur at reaction 1 or 3 (**Fig. 1**). We thus evaluated the impact of Ybp1·$Yap1^{SSS\ SSS}$ on reaction 1, using $Orp1^{CSA}$, which accumulates as a sulfenylamide at acidic pH upon conversion of the Orp1—SOH form (see above), and in the absence of Trx. Reaction products of Orp1 with excess H_2O_2 were analyzed as in **Fig. 4.** The major

chromatographic peaks observed were those of Yap1$^{SSS\ SSS}$ (peak 9), the Orp1^{CSA} sulfenylamide (peak 3) and reduced (peak 4) forms (**Fig. 5a**). Evolution of peak 3 area yielded first-order rate constants of 29 ± 7 s^{-1} in the absence of Yap1$^{SSS\ SSS}$ and Ybp1, and of 32 ± 7 and 24 ± 7 s^{-1} in their presence at a 1:1 ratio, and at 15 and 75 μM (**Fig. 5b**), respectively, which indicated that Orp1—SOH formation is not altered within the ternary complex (see also **Supplementary Fig 7d**).

We similarly measured the effects of the Ybp1·Yap1 complex on reaction 3, using Wt Orp1, and setting its catalytic cycle to single turnover to accumulate $Orp1_{OxSS}$, i.e. in the absence of the Trx system. Chromatographic analysis of the reaction mixtures identified Yap1$^{SSS\ SSS}$ (peak 9), $Orp1_{OxSS}$ (peak 7), reduced Orp1 (peak 8), and a small amount of a species with a mass that could not be determined (peak 10) (**Fig. 5c, Supplementary Table 2**). With Orp1 alone, evolution of peak 7 gave an observed rate constant of 32 ± 6 s^{-1}, close to the value measured for Orp1—SOH formation, which indicates that reaction 1 is limiting $Orp1_{OxSS}$ formation under these conditions (**Fig. 5d**). In contrast, in the presence of a 1:1 ratio of Yap1$^{SSS\ SSS}$ and Ybp1, evolution of peak 7 area now yielded a value of 10 ± 2 s^{-1} at 15 μM, and of 6 ± 2 s^{-1} at 75 μM of added proteins, indicating that in the ternary complex the rate-limiting step for $Orp1_{OxSS}$ formation switches from reaction 1 to reaction 3 (**Fig. 5d**). To further evaluate this effect, we determined reaction 3 intrinsic rate constant (k_{SS}) by monitoring the change of enzyme Trp fluorescence associated with C36-C82 disulfide formation, under single turnover conditions. We increased the concentration of H_2O_2 up to levels ensuring that reaction 1 is not rate-limiting relative to reaction 3 (**Supplementary Fig. 7**). The deduced value of k_{SS} for Orp1 alone, 507 ± 4 s^{-1}, was 80-fold higher than the 6 s^{-1} measured in the presence of Ybp1 and Yap1$^{SSS\ SSS}$. Accordingly, reaction 3 rate constant (k_{SS}) is > 1000-fold higher than the observed value of reaction 2 in the absence of Ybp1 (0.3 s^{-1}) (**Fig. 4**). In the presence of Ybp1 alone, the value of k_{SS} decreased to 22 s^{-1}, indicating a large contribution of Ybp1 to the slowdown of reaction 3 within the ternary complex (**Supplementary Fig. 7d**).

We therefore enquired whether eliminating the Orp1 resolving Cys residue would make Ybp1 dispensable for Yap1 oxidation. In cells that express Orp^{C82S}, oxidation of Yap1 by H_2O_2 is not

altered[9]. In Δ*ybp1* cells, Orp1^{C82S} did not allow Yap1 oxidation, even when overexpressed, although in the latter condition a very faint band corresponding to the Orp1-Yap1 disulfide-linked complex could now be seen (**Fig. 6a,b, Supplementary Fig. 11)**. *In vitro* also, Orp1^{C82S} did not allow Yap1 oxidation in the absence of Ybp1, but instead totally shifted Yap1 into several high molecular weight (HMW) species (**Fig. 6c).** These species were formed by the independent attachment of more than three Orp1^{C82S} molecules to Yap1, as deduced from the presence of a unique such attachment when Orp1^{CSA} was reacted with Yap1^{SSSCSS} (**Supplementary Fig. 6a**). These Orp1-Yap1 HMW species decreased upon reintroducing Ybp1 (**Fig. 6c**), with the very few remaining caused by excess free Orp1 that had reacted with Yap1 in an Ybp1-independent manner, as shown by the titration of Ybp1·Yap1 by Orp1 (**Supplementary Fig. 6b**).

We lastly enquired whether glutathione (GSH) at physiological concentrations would compete with Yap1 for condensation with Orp1—SOH. In the absence of Ybp1, GSH totally prevented the reaction between Orp1^{CSA} and Yap1^{SSSCSS}, and in its presence, it prevented this reaction only when Orp1^{CSA}, but not Wt Orp1 was used (**Supplementary Fig. 12)**. This effect of GSH most probably occurs on the free unassembled fraction of Yap1. Hence, a competition between GSH and Yap1 for condensation with Orp1—SOH C598 is prevented by ternary complex formation, which explains why GSH does not interfere with Yap1 activation *in vivo*, and why the Orp1^{C82S} mutant has a Wt phenotype with regards to Yap1 activation[9].

Hence, within the ternary complex, reaction of the Orp1—SOH with one (C598) out of the five others Yap1 Cys residues is specified, which adds to the activation of reaction 2 and to the impediment of reaction 3 within this complex, and the accessibility of GSH is prevented. In conclusion, the different levels at which Ybp1-dependent ternary complex formation improves H_2O_2 signaling from Orp1 to Yap1 explain why Ybp1 cannot be made dispensable under any conditions.

DISCUSSION

Since the identification of Orp1 as the H_2O_2 receptor in Yap1 activation[9], other thiol-peroxidases-based redox relays have been recognized [16,17,24–26]. Due to the high reactivity of its peroxidatic Cys residue, Orp1 confers to the Yap1 redox relay H_2O_2 specificity and sensitivity, i.e. the ability to detect very low doses of peroxide and to remain unreactive to other oxidants[2]. How then is achieved the functional coupling between Orp1 and Yap1 and what are the mechanisms ensuring absolute precision in the transfer of H_2O_2 oxidizing equivalents? Formation of a sulfenic acid at the Orp1 catalytic Cys residue upon its reaction with H_2O_2 initiates the first step of the redox relay, i.e. formation of the Orp1—S—S—Yap1 species. Based on estimates of the cellular concentrations of Orp1 of ~ 0.5 µM, and of Yap1 below 0.1 µM[27,28], and on the bimolecular rate constant measured here (7.4 10^3 $M^{-1}.s^{-1}$), formation of the Orp1—S—S—Yap1 complex would require > 10 min, which is not consistent with Yap1 fast oxidation *in vivo*. Furthermore, Orp1 peroxidatic turnover involves formation of an intramolecular disulfide between the same Cys-sulfenic acid and the Orp1 resolving Cys residue at a rate that should totally impede formation of the Orp1-Yap1 intermolecular disulfide. We show here, that Ybp1, a protein identified as a Yap1-binding partner with no recognizable functional domains, and then as required for its oxidative activation[13], enables the redox coupling between Orp1 and Yap1 at several levels. By recruiting these two proteins within a ternary complex, Ybp1 raises their local concentration, thereby increasing the rate constant for their reaction from the predicted value in the 10^{-3} s^{-1} to the 1 s^{-1}, even for the estimated low *in vivo* concentrations of the three partners (see details in **Supplementary Fig. 9**). *In vitro* reconstitution also shows that by enabling the recruitment of the peroxide-sensitive Orp1 factor, Ybp1 decreases by more than 50-fold the concentration of H_2O_2 needed to oxidize Yap1 (100 µM *vs*. >5 mM, **Supplementary Fig. 5**).

The previously described Orp1-dependent proximity-based oxidation of the redox protein roGFP2 by H_2O_2 was made possible by the fusion between these two proteins[29]. Ybp1 similarly enables Orp1-Yap1 redox coupling by ternary complex formation, but may also improve its

efficiency. Ternary complex formation might create a molecular environment that either stabilizes the C598 thiolate and/or provide the means of acid catalysis to activate the release of a water molecule, which is akin to an enzyme active site. In the absence of Ybp1, the Orp1-SOH could react with any of the Yap1 Cys residues (see **Fig. 6c**, and **Supplementary Fig. 6b**), which indicates that within the ternary complex both selection of C598 over the other five Yap1 Cys residues and its alignment with C36—SOH might also be favored. In addition, ternary complex formation appears also to prevent the attack of glutathione on the C36—SOH by impeding access of GSH to the sulfenic acid (**Supplementary Fig. 12**).

Lastly, our data indicate that the rate of attack of the resolving C82 thiolate on the Orp1—SOH that leads to $Orp1_{OxSS}$ formation is decreased by 20-fold within the Orp1·Ybp1 binary complex, and by > 80-fold within the Orp1·Ybp1·Yap1 complex, which are values in the range of those of reaction 2 (6 *vs* 5 s^{-1}). Therefore, within the ternary complex, the reaction between the Orp1—SOH and Yap1 C598 is activated, and the competing reaction between the Orp1-SOH and Orp1 C82 inhibited, which also favors the former. The failure of the Orp1 C82S mutant to activate Yap1 in the absence of Ybp1 underscores the fact that the inhibition of Orp1 intramolecular disulfide formation is just one of the means by which Ybp1-dependent ternary complex formation enables the redox relay. The Orp1 domain that comprises the C82 residue is highly flexible[30], which might allow it to be constrained within the ternary complex into a conformation preventing its reaction with the C36-SOH. Structural reorganization of Orp1 upon its interaction with Ybp1·Yap1 and Ybp1 is consistent with the significant entropic change associated with complex formation, as measured by ITC (**Supplementary Table 1**), and with the inability of $Orp1_{OxSS}$ to interact with Ybp1·Yap1 and Ybp1. Since Orp1 C82 residue is dispensable for Yap1 activation and since Orp1 peroxidase activity does not contribute to cellular H_2O_2 tolerance[9], why has evolution maintained the C82 residue? Based on the *in vivo* protein concentration estimates and on the dissociation constants for Orp1·Ybp1·Yap1 complex formation, a large fraction of Orp1 exists as a free protein. Therefore, free Orp1 fast disulfide formation might shield the reactivity of the Orp1—SOH, a hypothesis that is corroborated

by the *in vivo* identification of disulfide crosslinks between $Orp1^{C82S}$ and several proteins[31], while ensuring the availability of reduced Orp1 for Yap1 activation upon recycling of $Orp1_{OxSS}$ by Trx.

In summary we propose that Ybp1 acts as signaling scaffold, akin to the signaling scaffolds of GTPases, protein kinases and phosphatases[32], since it binds to two signaling proteins and helps guiding the flow of information between them. By shielding a protein Cys—SOH, and selectively activating its condensation into a disulfide with one over other thiolates, Ybp1 scaffolding function also incorporates the function of a "sulfenic acid chaperone", principles that may apply to other sulfenic acid-dependent signaling pathways.

ACKNOWLEDGMENTS

We gratefully acknowledge G. Branlant for his essential input to initiate the project. We also thank A. Gruez for assistance in protein stability optimization, S. Boschi-Muller and F. Talfournier for fruitful discussions and help with quench flow experiments, J.M. Alberto for support with use of NGERE U954-INSERM chromatographic facility, J. Charbonnel and G. Palais for excellent technical support. Microcalorimetry and mass spectrometry were performed respectively at SCBIM (Fédération de Recherche 3209 BMCT) and SCMS platforms of Université de Lorraine. This work was supported by grants from Ligue contre le Cancer to SRC, and from ANR ERRed, InCA PLBIO INCA_5869 to MBT. A.B. was supported by a PhD fellowship from the French research minister.

AUTHOR CONTRIBUTIONS

A.B., B.D.A., M.B.T. and S.R.C. designed the experiments and analyzed the data. A.B., A.K. and B.D.A. produced and purified the proteins, A.B. and B.D.A. performed *in vitro* reconstitution assays, B.D.A. on gels kinetics and A.B. all other kinetics, H.M. and A.B. chromatography and mass spectrometry analyses, A.B. and A.K. protein interaction experiments. G.B., B.D.A. and A.D.M. carried out *in vivo* experiments. S.R.C, B.D.A. and M.B.T wrote the manuscript.

REFERENCES

1. D'Autréaux, B. & Toledano, M. B. ROS as signalling molecules: mechanisms that generate specificity in ROS homeostasis. *Nat. Rev. Mol. Cell Biol.* **8,** 813–824 (2007).
2. Toledano, M. B., Delaunay, A., Monceau, L. & Tacnet, F. Microbial H_2O_2 sensors as archetypical redox signaling modules. *Trends Biochem. Sci.* **29,** 351–357 (2004).
3. Kuge, S. Regulation of yAP-1 nuclear localization in response to oxidative stress. *EMBO J.* **16,** 1710–1720 (1997).
4. Delaunay, A., Isnard, A.-D. & Toledano, M. B. H_2O_2 sensing through oxidation of the Yap1 transcription factor. *EMBO J.* **19,** 5157–5166 (2000).
5. Wood, M. J., Andrade, E. C. & Storz, G. The redox domain of the Yap1p transcription factor contains two disulfide bonds. *Biochemistry* **42,** 11982–11991 (2003).
6. Wood, M. J., Storz, G. & Tjandra, N. Structural basis for redox regulation of Yap1 transcription factor localization. *Nature* **430,** 917–921 (2004).
7. Kuge, S., Toda, T., Iizuka, N. & Nomoto, A. Crm1 (XpoI) dependent nuclear export of the budding yeast transcription factor yAP-1 is sensitive to oxidative stress. *Genes Cells* **3,** 521–532 (1998).
8. Yan, C., Lee, L. H. & Davis, L. I. Crm1p mediates regulated nuclear export of a yeast AP-1-like transcription factor. *EMBO J.* **17,** 7416–7429 (1998).
9. Delaunay, A., Pflieger, D., Barrault, M. B., Vinh, J. & Toledano, M. B. A thiol peroxidase is an H_2O_2 receptor and redox-transducer in gene activation. *Cell* **111,** 471–481 (2002).
10. Ma, L.-H., Takanishi, C. L. & Wood, M. J. Molecular mechanism of oxidative stress perception by the Orp1 protein. *J. Biol. Chem.* **282,** 31429–31436 (2007).
11. Paulsen, C. E. & Carroll, K. S. Chemical dissection of an essential redox switch in Yeast. *Chem. Biol.* **16,** 217–225 (2009).
12. Jencks, W. P. *Catalysis in Chemistry and Enzymology*, Ch 1 (Courier Corporation, 1987).

13. Veal, E. A., Ross, S. J., Malakasi, P., Peacock, E. & Morgan, B. A. Ybp1 is required for the hydrogen peroxide-induced oxidation of the Yap1 transcription factor. *J Biol. Chem.* **278,** 30896–904 (2003).
14. Gulshan, K., Lee, S. S. & Moye-Rowley, W. S. Differential oxidant tolerance determined by the key transcription factor Yap1 is controlled by levels of the Yap1-binding protein, Ybp1. *J. Biol. Chem.* **286,** 34071–34081 (2011).
15. Patterson, M. J. *et al.* Ybp1 and Gpx3 signaling in *Candida albicans* govern hydrogen peroxide-induced oxidation of the Cap1 transcription factor and macrophage escape. *Antioxid. Redox Signal.* **19,** 2244–2260 (2013).
16. Fomenko, D. E. *et al.* Thiol peroxidases mediate specific genome-wide regulation of gene expression in response to hydrogen peroxide. *Proc. Natl. Acad. Sci.* **108,** 2729–2734 (2011).
17. Sobotta, M. C. *et al.* Peroxiredoxin-2 and STAT3 form a redox relay for H_2O_2 signaling. *Nat. Chem. Biol.* **11,** 64–70 (2015).
18. Gupta, V. & Carroll, K. S. Sulfenic acid chemistry, detection and cellular lifetime. *Biochim. Biophys. Acta BBA - Gen. Subj.* **1840,** 847–875 (2014).
19. Devarie-Baez, N. O., Silva Lopez, E. I. & Furdui, C. M. Biological chemistry and functionality of protein sulfenic acids and related thiol modifications. *Free Radic. Res.* **50,** 172–194 (2016).
20. Tachibana, T. *et al.* A major peroxiredoxin-induced activation of Yap1 transcription factor is mediated by reduction-sensitive disulfide bonds and reveals a low level of transcriptional activation. *J. Biol. Chem.* **284,** 4464–4472 (2008).
21. Haynes, A. C., Qian, J., Reisz, J. A., Furdui, C. M. & Lowther, W. T. Molecular basis for the resistance of human mitochondrial 2-Cys peroxiredoxin 3 to hyperoxidation. *J. Biol. Chem.* **288,** 29714–29723 (2013).
22. Salmeen, A. *et al.* Redox regulation of protein tyrosine phosphatase 1B involves a sulphenyl-amide intermediate. *Nature* **423,** 769–773 (2003).

23. Lim, J. C., You, Z., Kim, G. & Levine, R. L. Methionine sulfoxide reductase A is a stereospecific methionine oxidase. *Proc. Natl. Acad. Sci.* **108,** 10472–10477 (2011).
24. Jarvis, R. M., Hughes, S. M. & Ledgerwood, E. C. Peroxiredoxin 1 functions as a signal peroxidase to receive, transduce, and transmit peroxide signals in mammalian cells. *Free Radic. Biol. Med.* **53,** 1522–1530 (2012).
25. Calvo, I. A. *et al.* Dissection of a redox relay: H_2O_2-dependent activation of the transcription factor Pap1 through the peroxidatic Tpx1-thioredoxin cycle. *Cell Rep.* **5,** 1413–1424 (2013).
26. Winterbourn, C. C. & Hampton, M. B. Redox biology: Signaling via a peroxiredoxin sensor. *Nat. Chem. Biol.* **11,** 5–6 (2015).
27. Ghaemmaghami, S. *et al.* Global analysis of protein expression in yeast. *Nature* **425,** 737–741 (2003).
28. Webster, M. T., McCaffery, J. M. & Cohen-Fix, O. Vesicle trafficking maintains nuclear shape in *Saccharomyces cerevisiae* during membrane proliferation. *J. Cell Biol.* **191,** 1079–1088 (2010).
29. Gutscher, M. *et al.* Proximity-based protein thiol oxidation by H_2O_2-scavenging peroxidases. *J. Biol. Chem.* **284,** 31532–31540 (2009).
30. Zhang, W.-J. *et al.* Crystal structure of glutathione-dependent phospholipid peroxidase Hyr1 from the yeast *Saccharomyces cerevisiae*. *Proteins Struct. Funct. Bioinforma.* **73,** 1058–1062 (2008).
31. Lee, P. Y. *et al.* Interactome analysis of yeast glutathione peroxidase 3. *J. Microbiol. Biotechnol.* **18,** 1364–1367 (2008).
32. Langeberg, L. K. & Scott, J. D. Signalling scaffolds and local organization of cellular behaviour. *Nat. Rev. Mol. Cell Biol.* **16,** 232–244 (2015).

FIGURE LEGENDS

435

436 **Figure 1 | Schematics of the dual function of Orp1 as the H_2O_2 receptor of the Yap1 regulator**
437 **and as a peroxidase** (adapted from ref. 1)**.** The Orp1-Yap1 redox relay is depicted at the right:
438 reaction of Orp1 catalytic Cys (C36) with H_2O_2 leads to reduction of the latter into H_2O and to
439 formation of the C36-sulfenic acid (C36-SOH) (reaction 1), which condenses with Yap1 C598 to
440 produce the Orp1—S—S—Yap1 intermediate (reaction 2). The latter is transposed into a Yap1
441 intramolecular disulfide by attack of Yap1 C303. Yap1 full activation requires further oxidation
442 reactions. Once formed, the C36-SOH condenses with Orp1 C82 into an intramolecular disulfide
443 ($Orp1_{OxSS}$) (reaction 3), which is then reduced by thioredoxin (Trx), completing the cycle. Reaction 2
444 and 3 are in competition.

445

446 **Figure 2 | Ybp1 brings together Yap1 and Orp1 into a ternary complex**. **(a)** Yap1 (30 µM, solid
447 line), Ybp1 (30 µM, dashed line), or both at a 1:1 (dotted line) or 2:1 (dashed-dotted line)
448 stoichiometry were resolved on a Superdex 200 gel filtration column equilibrated in 20 mM
449 Na_2HPO_4, 300 mM NaCl buffer pH 7. **(b)** Fluorescence anisotropy titration of AF-Ybp1 by Yap1
450 (square), AF-Yap1 by Ybp1 (circle) or AF-Ybp1 by $Yap1^{SSS\ SSS}$ (triangle). The fraction of bound-
451 labeled protein is plotted against unlabeled protein concentration and fitted to a single-site binding
452 equation (solid, dashed and dotted lines, respectively). The TCEP reducing agent had no effect on
453 the dissociation constant. **(c)** Isothermal titration calorimetry of $Yap1^{SSS\ SSS}$ (50 µM, left), or Ybp1 (20
454 µM, center) or both at 1:1 stoichiometric amounts (50:50 µM, right) by Orp1. In the latter
455 experiment, 85 % of Ybp1 and $Yap1^{SSS\ SSS}$ are bound together. Thermodynamic parameters
456 describing these interactions are in **Supplementary Table 1**. Data are representative of n=2
457 independent experiments using different proteins samples.

458

459 **Figure 3 | Ybp1 is required for Orp1—S—S—Yap1 intermediate formation. (a)** Extracts from
460 Wt or Δ*ybp1* cells carrying Myc-Yap1 orMyc-$Yap1^{C303A}$ and exposed or not to H_2O_2 (400 µM) for 15

min, as indicated, were resolved by non-reducing SDS-PAGE followed by anti-Myc immunoblotting. Yap1-Orp1 mixed disulfide (Orp1—S—S—Yap1), reduced ($Yap1_{red}$) and intramolecular disulfide ($Yap1_{ox}$) Yap1 species are indicated by arrows. **(b)** *In vitro* reconstitution of the Orp1/Yap1 redox relay. Coomassie-stained non-reducing SDS-PAGE of reaction mixtures containing Orp1 (10 µM), Yap1 (4 µM), Ybp1 (4 µM), Trx (4 µM), Trx reductase (0.5 µM) and NADPH (0.4 mM) incubated for the indicated time with H_2O_2 (60 µM). **(c)** As in (b) with reaction mixtures containing Orp1 (10 µM), Yap1 (2 µM), Trx (10 µM), Trx reductase (0.5 µM) and NADPH (1 mM) in the absence or presence of Ybp1 at the indicated amount relative to Yap1, incubated for the indicated time with H_2O_2 (2 mM). **(d)** As in (b) with reactions mixture containing Orp1 (10 µM) and $Yap1^{C303A}$ (2 µM), in the absence or presence of Ybp1 (2 µM) incubated for the indicated time with H_2O_2 (60 µM). Orp1 migrate outside gels in (b,c,d). MW, molecular weight (kDa). Data representative of n=2 or n=3 independent experiments. Complete gels are shown in **Supplementary Fig. 4.**

Figure 4 | Ybp1 activates Orp1—S—S—Yap1 formation. (a,c) $Orp1^{CSA}$ (a) or Orp1 (c) (50 µM), incubated with Ybp1 (10 µM) and $Yap1^{SSS\ CSS}$ (10 µM), were reacted with H_2O_2 (100 µM). **(e)** $Orp1_{OxSS}$ (50 µM) incubated with Ybp1 (10 µM) was reacted with $Yap1^{SSS\ CSS}$ (10 µM). Products were analyzed by reverse-phase chromatography after acidic quenching. Masses of products eluted are in **Supplementary Table 2**. Ybp1 was eluted at a higher acetonitrile ratio and does not appear on the chromatograms. **(b,d,f)** Evolution of the area of peak 2 (in a) or peak 6 (in c,e) corresponding to Orp1—S—S—Yap1 (squares) analyzed by a first-order mono-exponential kinetic model (solid line); data for $Orp1^{CSA}$ in the absence of Ypb1 (b, circles). **(d, inset)** Dependence of the rate constant of Orp1—S—S—Yap1 formation on Orp1 concentration analyzed as in (c). Data are representative of n=2 or n=3 independent experiments performed with different proteins samples.

Figure 5 | The Ybp1·Yap1 complex inhibits Orp1 intramolecular disulfide formation. (a,c) $Orp1^{CSA}$ (a) or Orp1 (c) (15 µM), incubated with $Yap1^{SSS\ SSS}$ (15 µM) and Ybp1 (15 µM) were reacted

with H_2O_2 (100 µM) and products were analyzed as in Fig. 4. Masses of the products eluted in each peak are collected in **Supplementary Table 2**. **(b,d)** Evolution of the area of peak 3 (Orp1 sulfenylamide) (in b) or peak 7 ($Orp1_{OxSS}$) (in d) (circles) analyzed by a first-order mono-exponential kinetic model (dashed line); data obtained in the absence (squares, solid line) and presence of $Yap1^{SSS\ SSS}$ (75 µM) and Ybp1 (75 µM) (triangles, dotted line). In the latter condition, 90% of Orp1 is associated with the ternary complex. The experiment performed in the absence and presence of $Yap1^{SSS\ SSS}$ and Ybp1 gave similar chromatographic profiles as in a and c, except for the lack of peak 9 ($Yap1^{SSS\ SSS}$) when using Orp1 alone. Data are representative of n=2 or n=3 independent experiments performed with different protein samples.

Figure 6 | Lack of Orp1 resolving C82 does not make Ybp1 dispensable for Yap1 oxidation. **(a,b)** Lysates of Δ*yap1* or Δ*yap1*Δ*ybp1* or Δ*yap1*Δ*ybp1*Δ*orp1* cells, as indicated, expressing Myc-Yap1 (a,b) and overexpressing $Orp1^{C82S}$ (b), and treated with of H_2O_2 (400 µM) during the indicated time, were resolved by non-reducing SDS-PAGE followed by western-blot with an anti-Myc antibody. Yap1 redox conformers are indicated by arrows. **(c)** Coomassie-stained non-reducing SDS-PAGE of reactions mixture containing $Orp1^{C82S}$ (10 µM) and Yap1 (2 µM), and Ybp1 (2 µM), as indicated, incubated for the indicated time with H_2O_2 (100 µM). HMW, high molecular weight complexes. MW, molecular weight (kDa). Data are representative of n=2 or n=3 independent experiments. Complete gels are shown in **Supplementary Fig. 11.**

ONLINE METHODS

Chemicals

All chemicals were reagent grade and were used without additional purification. KCl, Ethylene diamine tetra acetic acid (EDTA), acetonitrile and Benzonase nuclease were purchased from Merck. Glucose and lactose were from Fisher Chemical. NaCl, sodium phosphate dibasic (Na_2HPO_4) were obtained from Carlo Erba Reagents. Hepes free acid was from MP Biomedicals. Tris, ammonium sulfate, isopropyl-β-D-thiogalactopyranoside (IPTG), chloramphenicol, ampicillin and kanamycin were from Euromedex. Trifluoroacetic acid (TFA) and H_2O_2 were obtained from Acros Organics. Sodium dodecyl sulfate (SDS) was obtained from AppliChem GmbH. N-ethylmaleimide (NEM), iodoacetamide (IAM), tris(2-carboxyethyl)phosphine (TCEP), mes, imidazole, betaine and phenylmethanesulfonylfluoride (PMSF), *E. coli* thioredoxin 2 (Trx) were from Sigma-Aldrich. *E. coli* thioredoxin reductase (Trx reductase) was from Sigma-Aldrich or prepared following experimental procedures described previously[33]. *E. coli* thioredoxin 1 (Trx1)[34], Methionine sulfoxide reductase (MsrA)[35] and *S. cerevisiae* peroxiredoxin Tsa1[36] were prepared following experimental procedures described previously.

Plasmids and Recombinant Protein Purification

The plasmids pET28bHTYap1 and pET28bHTYbp1 encoding the N-terminal His tag fusion of *S. cerevisiae* Yap1 (670 residues) and Ybp1 (674 residues), referred to as Yap1 and Ybp1 respectively, were obtained by cloning the Yap1 and Ybp1 ORFs amplified from *S. cerevisiae* genomic DNA by PCR into the pET28b and pET22b vectors, using the NdeI and SacI or NotI and SacI restriction sites, respectively. The plasmid pET22bOrp1 encoding *S. cerevisiae* Orp1 (163 residues) was obtained similarly by cloning the Orp1 ORF into the pET22b vector, using the NdeI and SacI sites. All mutant of Yap1 and Orp1 were generated by standard PCR site-directed mutagenesis and sequenced to confirm that no mutations had been introduced in the amplification reactions.

Wt and mutant Yap1 and Ybp1 were overexpressed in *E. coli* Rosetta 2(DE3) strain (Novagen) transformed by the pET28bHTYap1 and pET28bHTYbp1, respectively. For Yap1 production, cells were grown for 5 h at 37° C in Luria-Bertani (LB) medium supplemented by and 0.5% glucose, followed by addition of 1:1 volume of cold LB medium containing 0.6% lactose, 20 mM Hepes pH 7, 1 mM IPTG, kanamycin (50 $mg.l^{-1}$) and chloramphenicol (50 $mg.l^{-1}$) and further incubation for 18 h at 20° C. For Yap1 purification, cells pellets were suspended in 20 mM Na_2HPO_4 pH8 buffer, 400 mM NaCl (buffer A), supplemented by 1 mM PMSF, Roche protease EDTA free inhibitor cocktail (Roche Applied Science, Indianapolis, IN) and 5 U.ml-1 Benzonase nuclease and lysed by sonication. Yap1 contained in the soluble fraction was purified on Ni^{2+}-sepharose column (GE Healthcare) equilibrated with buffer A with 60 mM imidazole, connected to a fast protein liquid chromatography (FPLC) system (ÄKTA Avant, GE Healthcare), and eluted with a linear 0.06 to 0.5 M imidazole gradient. Fractions containing Yap1 were dialyzed against 20 mM Na_2HPO_4, 100 mM NaCl, pH 8 containing 20 mM DTT, and further purified on a anion exchange Q-sepharose column (GE Healthcare) equilibrated in the same buffer, using a linear gradient of 0.1 to 1 M NaCl.

For Ybp1 production, cells were grown in LB medium containing kanamycin (50 $mg.l^{-1}$), chloramphenicol (50 $mg.l^{-1}$) for 3 h at 37°C, followed by addition of 0.5 M NaCl and 2 mM betaine and incubation for 1h at 47°C (adapted from **ref. 37**[37]). Cells were then cooled to 20°C, and Ybp1 expression was induced by addition of 1 mM IPTG and incubation for 18h at 20°C. The same procedure as for Yap1 was used for Ybp1 purification on Ni^{2+}-sepharose column, except that buffer A was replaced by 20 mM Hepes, 400 mM NaCl, pH 8.5 buffer. Fractions containing Ybp1 were directly concentrated using an Amicon Ultra 30kDa concentrator before further purification by gel filtration on a Superdex 200 column (GE Healthcare) equilibrated in the same buffer.

Wt and mutants Orp1 were overexpressed in *E. coli* C41(DE3) strain transformed by the pET22bOrp1 plasmid by overnight culture at 37°C in the autoinducible media ZYM-5052 supplemented with ampicillin (200 $mg.l^{-1}$)[38]. For Orp1 purification, cells pellets were suspended in 50 mM Tris, 2 mM EDTA buffer pH 8 supplemented by 1 mM PMSF, 5 U/mL Benzonase Nuclease, 20

mM DTT and lysed by sonication. Orp1 contained in the soluble fraction was precipitated by ammonium sulfate at 65% saturation, followed by gel filtration on an Ultrogel AcA54 column (Biosepra, Pall Corporation). Fractions containing Orp1 were buffer exchanged by 20 mM Mes, 2 mM EDTA, pH 6.1 and further purified on a cation exchange SP-Sepharose column (GE Healthcare) equilibrated in the same buffer and eluted using a 0 to 1 M KCl gradient.

The identity and purity of Yap1, Ybp1 and Orp1 proteins were confirmed by Coomassie stained sodium dodecyl sulfate-polacrylamide gel electrophoresis (SDS-PAGE) and by electrospray mass spectrometry analyses. Purified proteins were stored at -80°C. Protein molar concentrations were determined spectrophotometrically using molar absorption coefficient at 280 nm of 30 285 $M^{-1}.cm^{-1}$, 69 680 $M^{-1}.cm^{-1}$ and 19 300 $M^{-1}.cm^{-1}$ for Yap1, Ybp1 and Orp1 respectively. Immediately before use, proteins were reduced by 20 mM DTT for 30 min at 4°C, followed by desalting against 20 mM Na_2HPO_4, 300 mM NaCl, pH7 (buffer B) degassed under nitrogen. $Orp1_{OxSS}$ was obtained by addition of 1.2 molar excess of H_2O_2 in Orp1 solution.

S. cerevisiae protein extracts and redox Western blots

Myc-Yap1, a N-terminal Yap1 fusion with a Myc_9 epitope and its mutant alleles inserted into a pRS315 vector were previously described[4]. The *S. cerevisiae* strain YPH98[39] (MATa, ura3-52, lys2-801amber, and ade2-101ochre trp1-Δ1 leu2-Δ1) and isogenic derivatives were used in all experiments. The Δ*ybp1* strain was derived from the WT strains by replacing the entire ORF by a KAN selection cassette. Δ*ybp1* strain transformed with pRS315-Myc-$Yap1^{C303A}$ were grown at 30°C in YPD [1% yeast extracts, 2% bactopeptone, and 2% glucose]. For overexpression of the $Orp1^{C82S}$ mutant, the Δ*ybp1* strain was transformed with pRS315-Myc-Yap1 and pRS426-$Orp1^{C82S}$ and the cells were grown in SD medium (0.67% Yeast Nitrogen Base without amino acid and 2% Glucose) with the required amino acids. For analysis of the *in vivo* Yap1 redox state, extracts were prepared by the TCA acid lysis method as described[4]. Precipitated proteins were solubilized in buffer containing 100 mM Tris-HCl pH 8, 1% SDS, 1 mM EDTA, and 50 mM NEM at 30°C for 1h (cysteine-

583 trapping method). Extracts were resolved by non-reducing 8% SDS-PAGE as indicated and analyzed
584 by immunoblotting with the anti-Myc monoclonal antibody (9E10) used at 1/2000°.
585
586 **SDS-PAGE analyses**
587 Reaction mixtures containing Yap1, Orp1 and their respective mutants, Ybp1, Trx, Trx
588 reductase, NADPH and H_2O_2 were incubated in Hepes 50 mM, NaCl 50 mM, EDTA 1 mM, pH = 7.5 at
589 room temperature and quenched with 100 mM IAM and 1% SDS at room temperature for 1 h.
590 Proteins were loaded onto 10% non-reducing SDS-PAGE gel (30:0.4 acrylamide:bisacrylamide),
591 followed by colloidal Coomassie staining (adapted from **ref. 40**[40]).
592
593 **Fluorescence anisotropy titrations**
594 The N-terminal amine of Ybp1 and Yap1 was derivatized in 20 mM Na_2HPO_4, 300 mM NaCl,
595 pH 8 by incubation with a tenfold molar excess of the fluorophore Alexa Fluor 488
596 sulfodichlorophenol Ester (Molecular probes, Life technologies) for 30 min at room temperature in
597 the dark. The labeled protein (AF-Yap1 or AF-Ybp1) was separated from excess dye by a Econo-Pac
598 10DG Desalting column (Bio-Rad). The protein concentration and the degree of labeling (typically
599 0.7-0.8 mol Alexa Fluor per mol of protein) were determined by UV-VIS spectroscopy.
600 Fluorescence intensity and anisotropy measurements were carried out on a
601 spectrofluorimeter SAFAS Flx-Xenius equipped with dual monochromators. The dissociation
602 constant of the Yap1·Ybp1 complex in buffer B at 25°C in the presence of 2 mM TCEP was deduced
603 from anisotropy titrations of 100 nM of AF-Ybp1 of AF-Ybp1 with increasing concentrations of Yap1
604 or Ybp1, respectively, recorded using 494 nm excitation and 523 nm emission wavelengths and 10
605 nm slits. The instrument computed anisotropy data from samples illuminated with vertically
606 polarized light $A = (I_{VV} - G.I_{VH})/(I_{VV} + 2G.I_{VH})$ where I_{VV} is the fluorescence intensity recorded with
607 excitation and emission polarization in vertical position, and I_{VH} is the fluorescence intensity
608 recorded with the emission polarization aligned in horizontal position. The G-factor of the

609 spectrofluorometer represents the ratio of the sensitivities of the detection system for vertically and
610 horizontally polarized light and was calculated by the instrument for each individual sample.
611 Data obtained were expressed as the fraction of labeled protein in complex, taking into
612 account the effect of complex formation on the fluorescence intensity according to equation (1),
613
614 $$\text{Fraction of labeled protein in complex} = (A - Af) / ((Ab - A) \times (Ib/If) + (A - Af)) \quad (1)$$
615
616 where Af, If and Ab, Ib represent the anisotropy and fluorescence intensity of free and complexed
617 labeled protein, respectively. Plots of the fraction of labeled protein in complex vs. unlabeled protein
618 concentration were fit to a single-site binding model to deduce Yap1·Ybp1 dissociation constant.
619 Dissociation constants are reported as the mean value obtained from n=2 independent experiments
620 performed on distinct protein productions ± standard deviation.
621
622 **Isothermal Titration Calorimetry**
623 ITC titration were performed using an iTC200 system from Microcal (GE Healthcare) at 25°C
624 in buffer B. Orp1 or $Orp1_{OxSS}$ (200 to 500 µM) contained in the syringe was injected into the sample
625 cell containing $Yap1^{SSS\ SSS}$, Ybp1 or an equimolar mix of both proteins (20 or 50 µM, as indicated), in
626 20 injections of 2 µL separated by delay of 180 s. Cell stirring speed was 750 rpm. Reference
627 injections of protein into buffer and buffer into protein were performed and subtracted from the
628 integrated data prior to curve fitting. Data were fit to a single-site binding model using Origin 7.0
629 software (Origin Labs) to determine the dissociation constant, enthalpy of binding (ΔH), and
630 stoichiometry. These parameters are reported as the mean value obtained from n=2 independent
631 experiments performed on distinct protein productions ± standard deviation.
632
633 **Stopped flow and quench flow rapid kinetics**

The reaction of Orp1 with H_2O_2 in single turnover conditions was followed by the increase of Orp1 intrinsic fluorescence intensity when oxidized to the $Orp1_{OxSS}$ disulfide form. Emission fluorescence was recorded at 25°C in buffer B on an SX19MV-R stopped flow apparatus (Applied Photophysics) fitted for fluorescence measurements, with excitation wavelength set at 295 nm, and emitted light collected above 320 nm using a cutoff filter. One syringe contained Orp1 (2 µM, final concentration after mixing), the other syringe contained H_2O_2. Equal volumes of each syringe were rapidly mixed to start the reaction. An average of at least three runs was recorded for each concentration of H_2O_2. The data set obtained at variable H_2O_2 concentrations was fitted globally to a two step process using Kintek Global Kinetic Explorer software to extract the rate constants k_{SOH} for Orp1—SOH formation and k_{SS} for $Orp1_{OxSS}$ formation.

To monitor the formation of the Orp1—S—S—Yap1 species, $Yap1^{SSS\ CSS}$, Orp1 in the presence or absence of Ybp1 were rapidly mixed with 100 µM H_2O_2 (final concentration after mixing) at room temperature in buffer B and incubated for defined reaction times (2.5 ms to 200 s) on a RQF3 chemical quenched-flow apparatus (Kintek corp., Austin, Texas). The reaction was then quenched by addition of 1 volume of 1% TFA and reaction products were analyzed by reversed-phase liquid chromatography (UltiMate 3000 Standard, Dionex) on an Vydac C8 300A (C8) column, 4,6x250 mm, 5 µm (Grace) equilibrated in 0.1% TFA. Proteins were eluted using a 20 min linear gradient of 35% to 41% acetonitrile at a flow rate of 2 $ml.min^{-1}$. Each species was identified by mass spectrometry. The rate constant of Orp1—S—S—Yap1 formation was deduced from the evolution of amount of product proportional to the area of the chromatographic peak. The rate constant of Orp1—S—S—Yap1 formation by reaction of $Orp1_{OxSS}$ was measured similarly by rapidly mixing $Orp1_{OxSS}$ and with $Yap1^{SSS\ CSS}$ in the presence of Ybp1. Rate constants are reported as the mean value obtained from n=2 or n=3 independent experiments performed on distinct protein productions ± standard deviation.

The kinetics of formation of $Orp1_{OxSS}$ and Orp1—SOH were monitored by the same protocol using either Wt Orp1 or $Orp1^{CSA}$, respectively, in the presence of equimolar mix of $Yap1^{SSS\ SSS}$ and Ybp1 at the indicated concentrations.

Steady-state kinetics

Orp1 peroxidase activity was measured by using the Trx/Trx reductase coupled (0.5 µM NTR, 250 µM NADPH, 50 µM Trx1), with 100 µM H_2O_2 and was started by addition of 0.05 µM Orp1 in buffer B at 25°C. Initial rate measurement were carried out on a UV mc2 spectrophotometer (Safas, Monaco) by following the decrease of absorbance at 340 nm due to the oxidation of NADPH. A blank measurement recorded in the absence of Orp1 was systematically deduced from the assay to account for non-specific oxidation of Trx or Trx reductase. Initial rate measurements were carried with Orp1 alone and in the presence of increasing concentrations of the proteins $Yap1^{SSS\ CSS}$, Ybp1 or an equimolar mix of both as indicated.

The Tsa1 peroxidase and the MsrA methionine sulfoxide reductase activities were measured by the same coupled assay using 100 µM H_2O_2 and 100 mM oxidized Met as substrate, respectively. Concentrations of the Trx recycling system were: 1 µM Trx reductase, 200 µM NADPH, 50 µM Trx1 and 0.5 µM Tsa1, and 4.8 µM Trx reductase, 200 µM NADPH, 100 µM Trx1 and 1 µM MsrA.

Mass spectrometry

Electrospray ionization mass spectrometry measurements were performed on a MicrOTOF-Q instrument (Bruker Daltonics) as described previously[41].

Data availability

The datasets generated and analysed during the current study are available from the corresponding authors on reasonable request.

33. Mulrooney, S. B. Application of a single-plasmid vector for mutagenesis and high-level expression of thioredoxin reductase and its use to examine flavin cofactor incorporation. *Protein Expr. Purif.* **9,** 372–378 (1997).
34. Mössner, E., Huber-Wunderlich, M. & Glockshuber, R. Characterization of *Escherichia coli* thioredoxin variants mimicking the active-sites of other thiol/disulfide oxidoreductases. *Protein Sci. Publ. Protein Soc.* **7,** 1233–1244 (1998).
35. Boschi-Muller, S. *et al.* A sulfenic acid enzyme intermediate is involved in the catalytic mechanism of peptide methionine sulfoxide rductase from *Escherichia coli*. *J. Biol. Chem.* **275,** 35908–35913 (2000).
36. Roussel, X. *et al.* Evidence for the formation of a covalent thiosulfinate intermediate with peroxiredoxin in the catalytic mechanism of sulfiredoxin. *J. Biol. Chem.* **283,** 22371–22382 (2008).
37. Oganesyan, N., Ankoudinova, I., Kim, S.-H. & Kim, R. Effect of osmotic stress and heat shock in recombinant protein overexpression and crystallization. *Protein Expr. Purif.* **52,** 280–285 (2007).
38. Studier, F. W. Protein production by auto-induction in high density shaking cultures. *Protein Expr Purif* **41,** 207–34 (2005).
39. Sikorski, R. S. & Hieter, P. A system of shuttle vectors and yeast host strains designed for efficient manipulation of DNA in *Saccharomyces cerevisiae*. *Genetics* **122,** 19–27 (1989).
40. Neuhoff, V., Arold, N., Taube, D. & Ehrhardt, W. Improved staining of proteins in polyacrylamide gels including isoelectric focusing gels with clear background at nanogram sensitivity using Coomassie Brilliant Blue G-250 and R-250. *Electrophoresis* **9,** 255–262 (1988).
41. Boukhenouna, S. *et al.* Evidence that glutathione and the glutathione system efficiently recycle 1-Cys sulfiredoxin in vivo. *Antioxid. Redox Signal.* **22,** 731–743 (2014).

COMPETING FINANCIAL INTERESTS

The authors declare no competing financial interests.

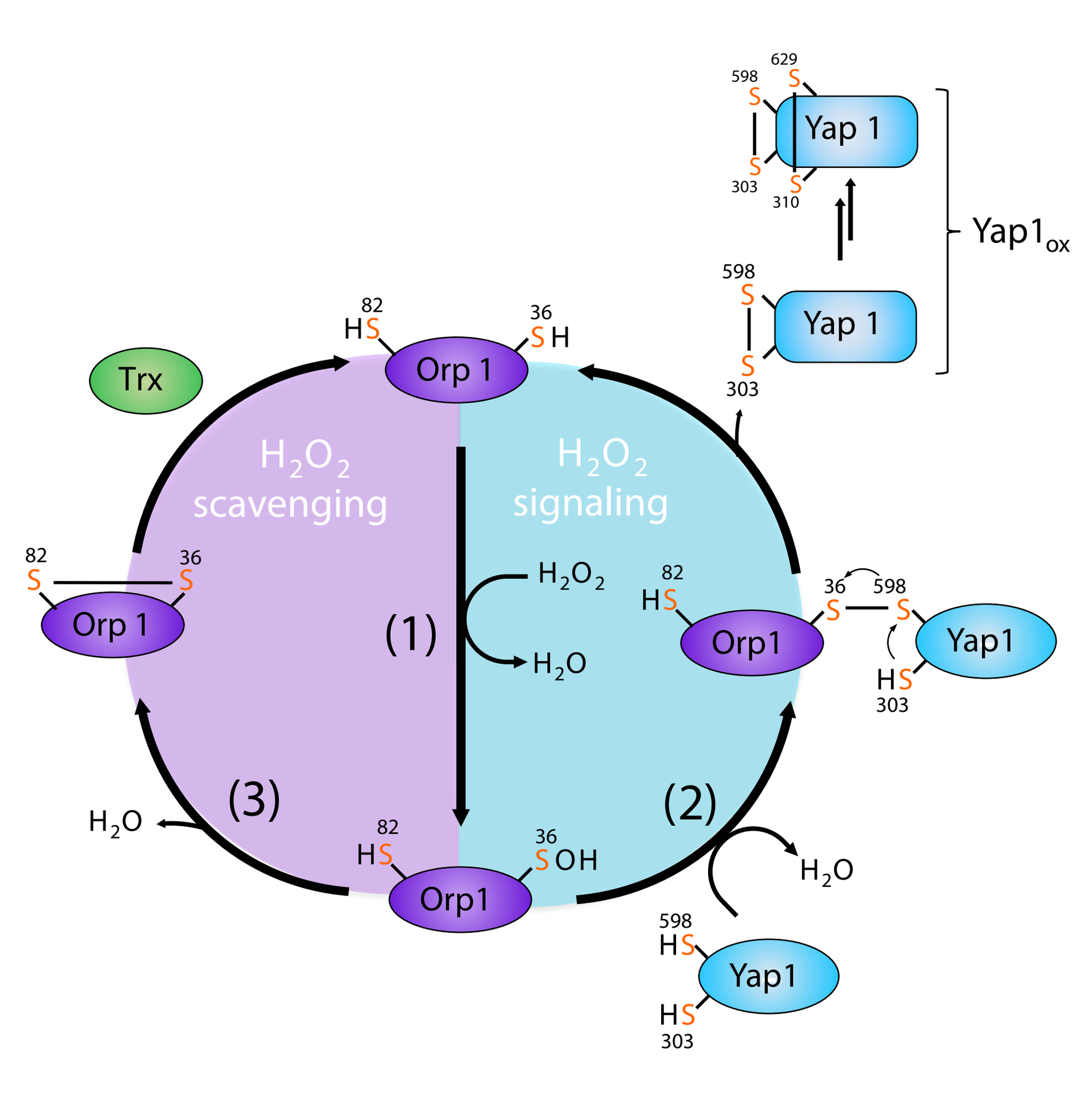
629
598
S
S
Yap 1
S
S
303
310
Yap1ox
598
S
S
Yap 1
303
82
HS
36
SH
Orp 1
Trx
H2O2
scavenging
H2O2
signaling
82
36
S
S
Orp 1
(1)
H2O2
H2O
82
HS
Orp1
36
598
S
S
Yap1
HS
303
(3)
(2)
H2O
H2O
82
HS
36
SOH
Orp1
598
HS
Yap1
HS
303

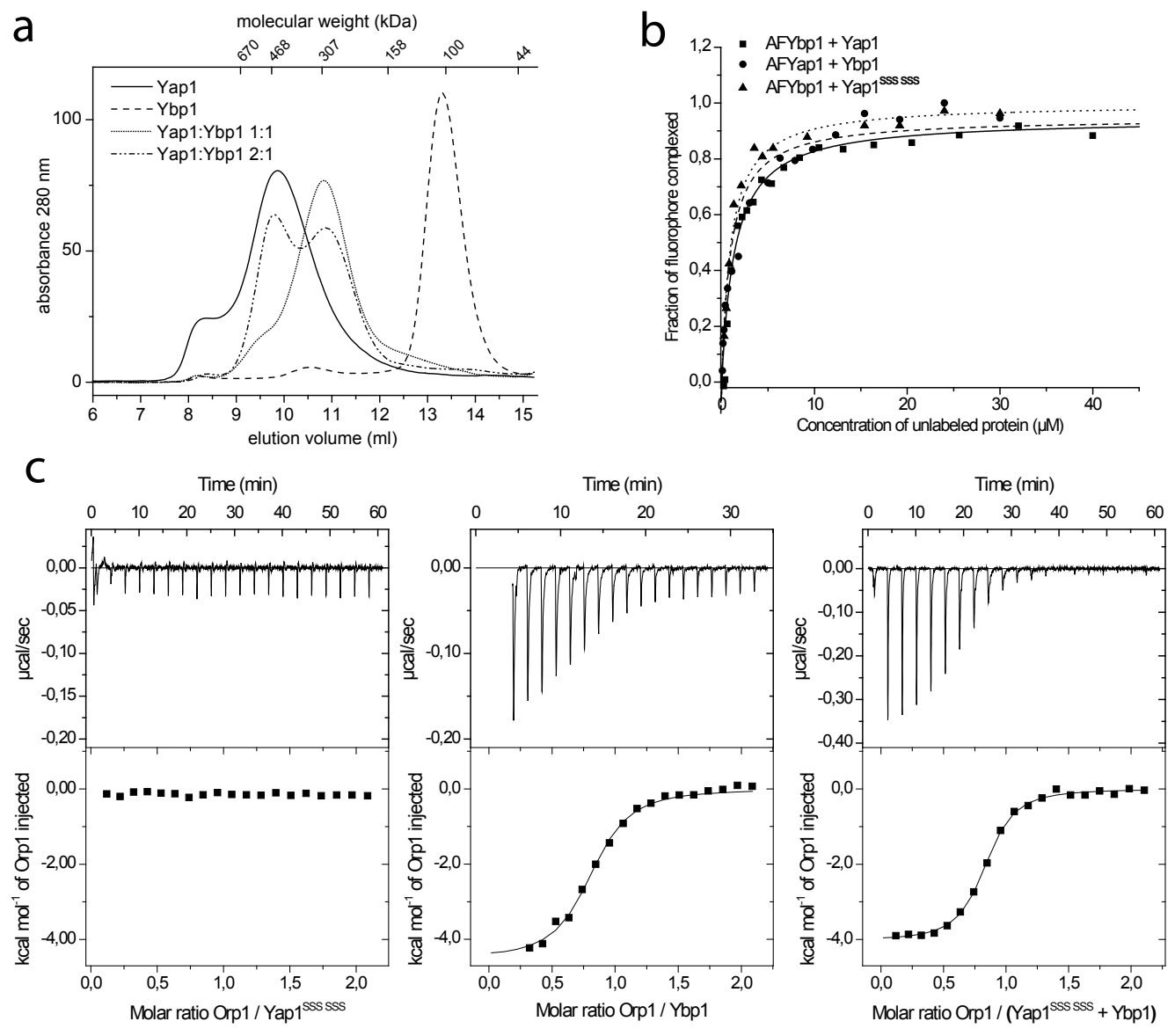
a
molecular weight (kDa)
670
468
307
158
100
44
Yap1
Ybp1
Yap1:Ybp1 1:1
Yap1:Ybp1 2:1
absorbance 280 nm
elution volume (ml)
b
AFYbp1 + Yap1
AFYap1 + Ybp1
AFYbp1 + Yap1SSS SSS
Fraction of fluorophore complexed
Concentration of unlabeled protein (μM)
c
Time (min)
μcal/sec
kcal mol-1 of Orp1 injected
Molar ratio Orp1 / Yap1SSS SSS
Molar ratio Orp1 / Ybp1
Molar ratio Orp1 / (Yap1SSS SSS + Ybp1)

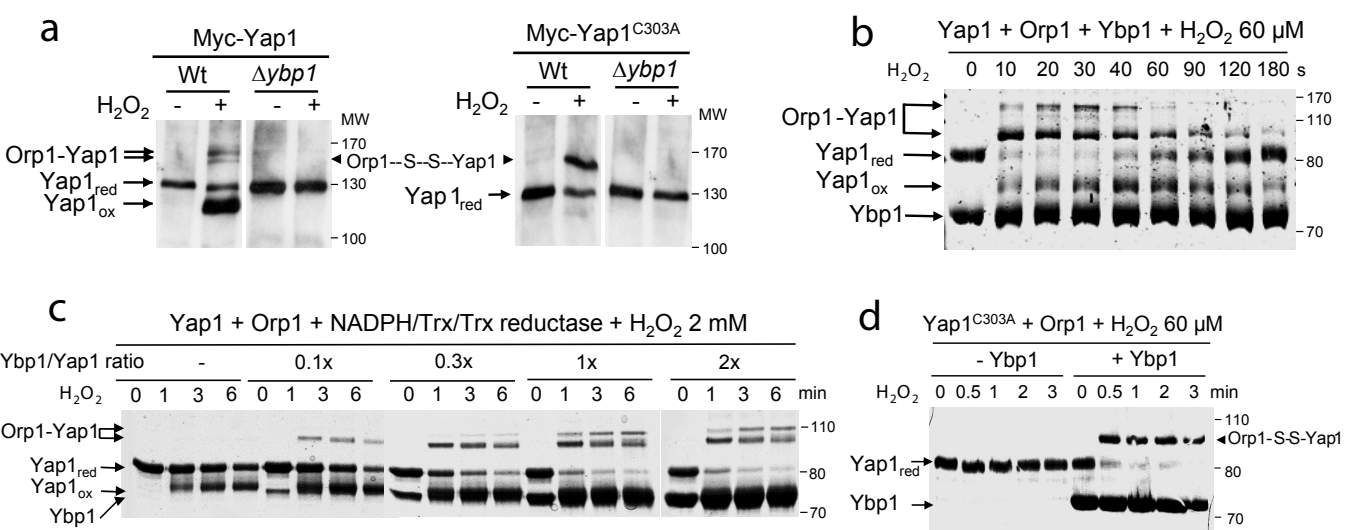
a
Myc-Yap1
Wt
Δybp1
H2O2
- + - +
MW
Orp1-Yap1
Yap1red
Yap1ox
170
130
100
Myc-Yap1C303A
Wt
Δybp1
H2O2
- + - +
MW
Orp1--S--S--Yap1
Yap 1red
170
130
100
b
Yap1 + Orp1 + Ybp1 + H2O2 60 μM
H2O2
0 10 20 30 40 60 90 120 180 s
Orp1-Yap1
Yap1red
Yap1ox
Ybp1
170
110
80
70
c
Yap1 + Orp1 + NADPH/Trx/Trx reductase + H2O2 2 mM
Ybp1/Yap1 ratio
-
0.1x
0.3x
1x
2x
H2O2
0 1 3 6 0 1 3 6 0 1 3 6 0 1 3 6 0 1 3 6 min
Orp1-Yap1
Yap1red
Yap1ox
Ybp1
110
80
70
d
Yap1C303A + Orp1 + H2O2 60 μM
- Ybp1
+ Ybp1
H2O2
0 0.5 1 2 3 0 0.5 1 2 3 min
Yap1red
Ybp1
110
Orp1-S-S-Yap1
80
70

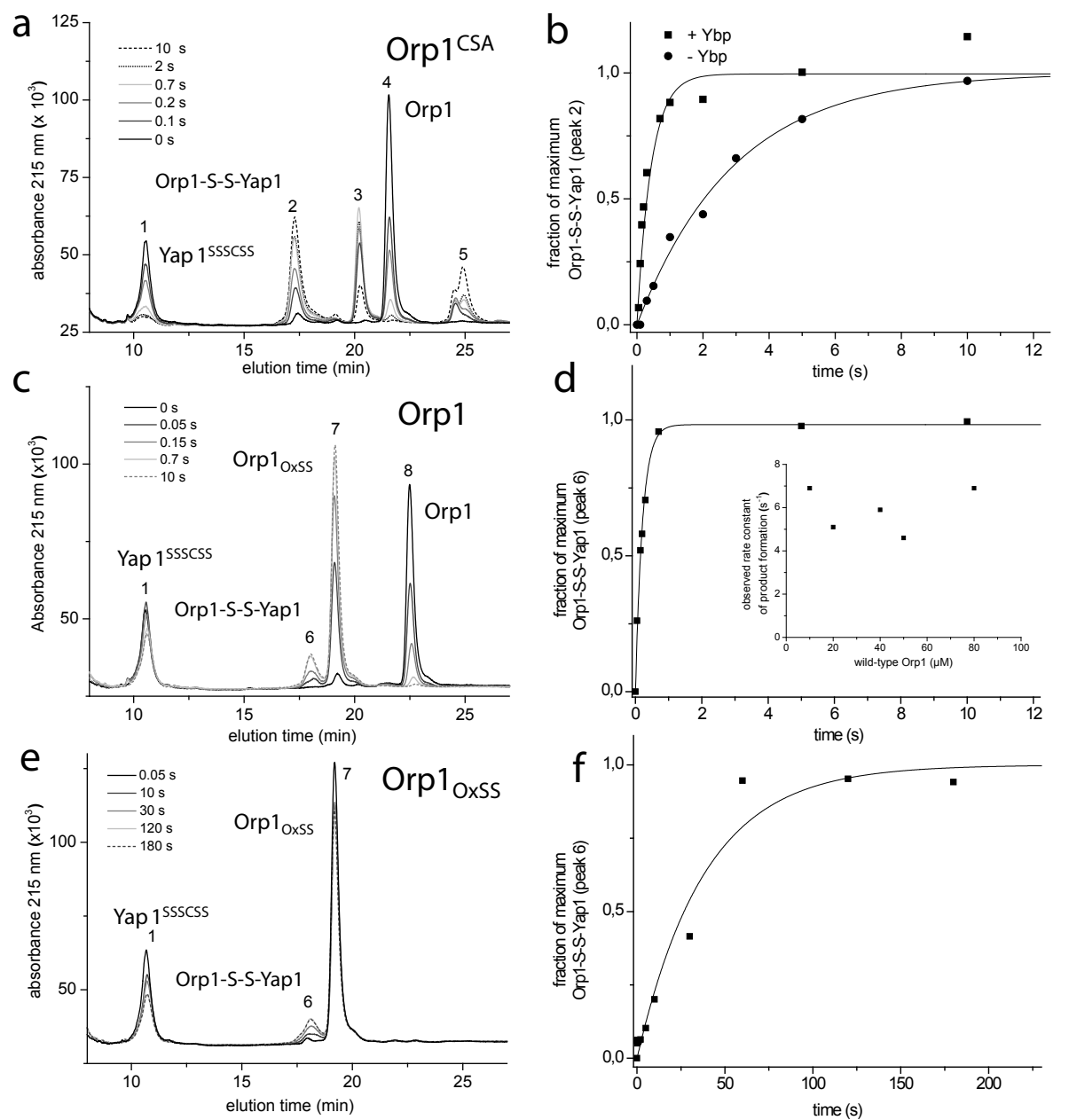
a
Orp1CSA
10 s
2 s
0.7 s
0.2 s
0.1 s
0 s
Orp1-S-S-Yap1
Yap 1SSSCSS
Orp1
absorbance 215 nm (x 10³)
elution time (min)
b
+ Ybp
- Ybp
fraction of maximum Orp1-S-S-Yap1 (peak 2)
time (s)
c
Orp1
0 s
0.05 s
0.15 s
0.7 s
10 s
Orp1OxSS
Yap 1SSSCSS
Orp1-S-S-Yap1
Orp1
Absorbance 215 nm (x10³)
elution time (min)
d
fraction of maximum Orp1-S-S-Yap1 (peak 6)
observed rate constant of product formation (s⁻¹)
wild-type Orp1 (μM)
time (s)
e
Orp1OxSS
0.05 s
10 s
30 s
120 s
180 s
Yap 1SSSCSS
Orp1-S-S-Yap1
absorbance 215 nm (x10³)
elution time (min)
f
fraction of maximum Orp1-S-S-Yap1 (peak 6)
time (s)

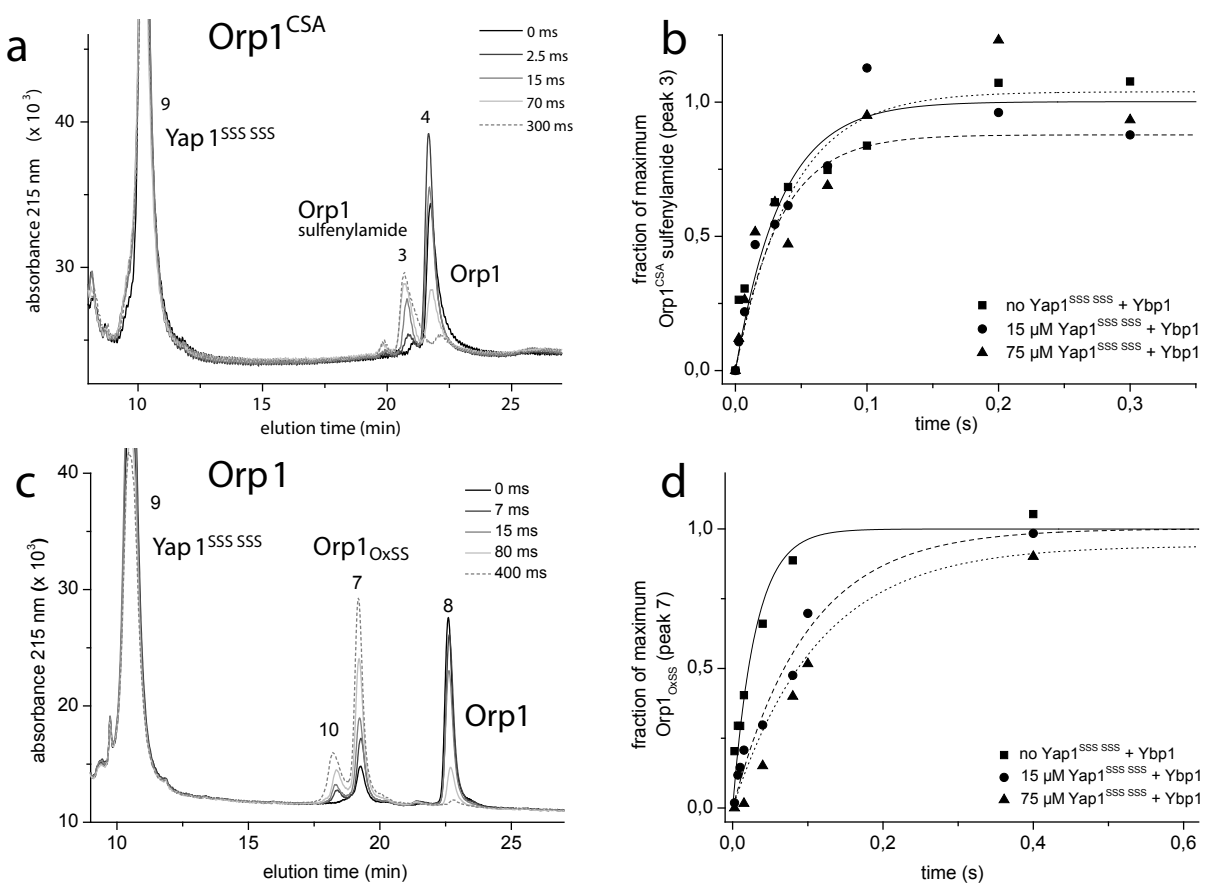
a
Orp1CSA
0 ms
2.5 ms
15 ms
70 ms
300 ms
9
Yap 1SSS SSS
4
Orp1
sulfenylamide
3
Orp1
absorbance 215 nm (x 10-3)
elution time (min)
b
fraction of maximum
Orp1CSA sulfenylamide (peak 3)
no Yap1SSS SSS + Ybp1
15 µM Yap1SSS SSS + Ybp1
75 µM Yap1SSS SSS + Ybp1
time (s)
c
Orp 1
0 ms
7 ms
15 ms
80 ms
400 ms
9
Yap 1SSS SSS
Orp1OxSS
7
8
10
Orp1
absorbance 215 nm (x 10-3)
elution time (min)
d
fraction of maximum
Orp1OxSS (peak 7)
no Yap1SSS SSS + Ybp1
15 µM Yap1SSS SSS + Ybp1
75 µM Yap1SSS SSS + Ybp1
time (s)

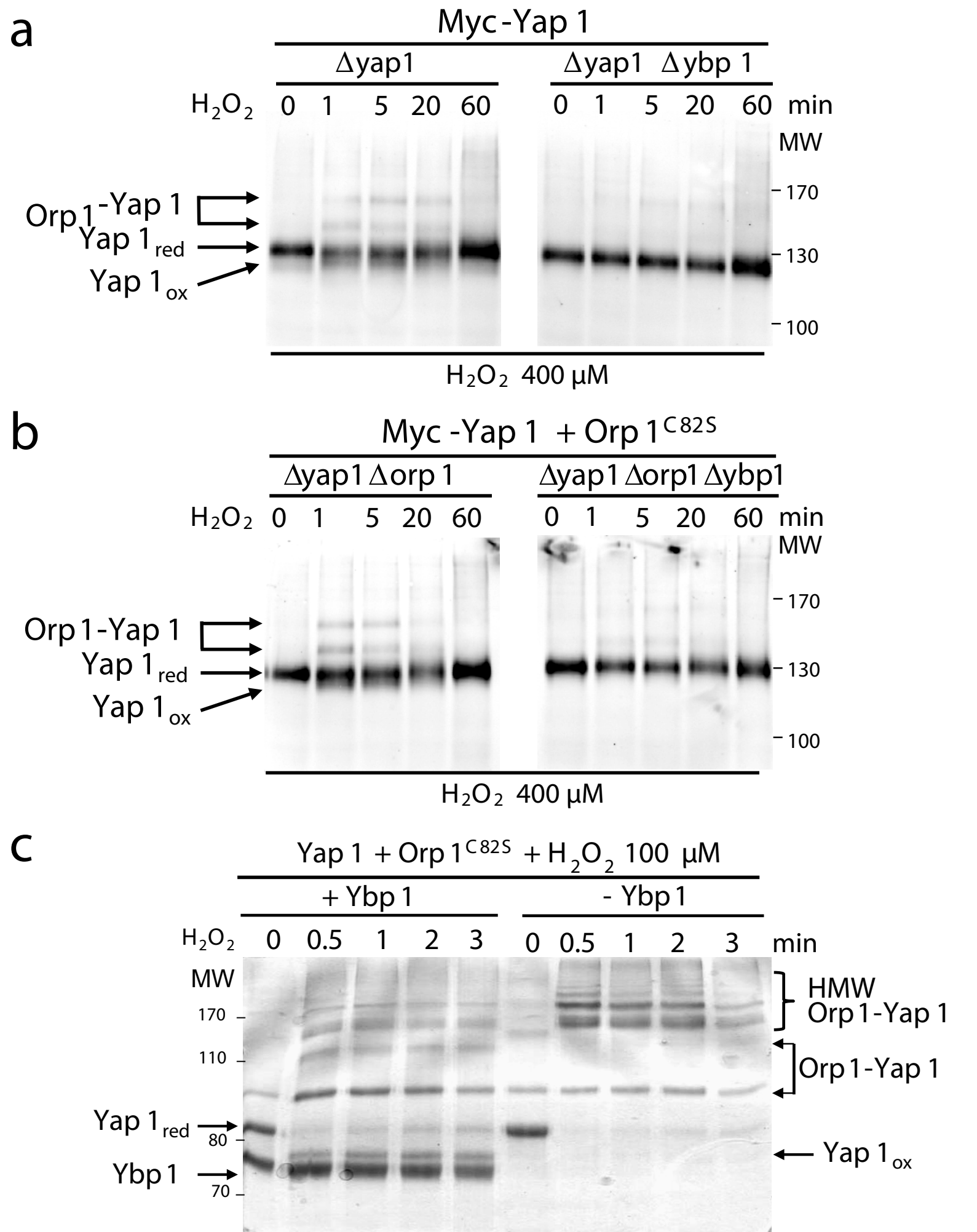
a
Myc-Yap 1
Δyap1
Δyap1 Δybp 1
H2O2
0 1 5 20 60
0 1 5 20 60 min
MW
170
130
100
Orp1-Yap 1
Yap 1red
Yap 1ox
H2O2 400 µM
b
Myc -Yap 1 + Orp 1C82S
Δyap1 Δorp 1
Δyap1 Δorp1 Δybp1
H2O2
0 1 5 20 60
0 1 5 20 60 min
MW
170
130
100
Orp1-Yap 1
Yap 1red
Yap 1ox
H2O2 400 µM
c
Yap 1 + Orp 1C82S + H2O2 100 µM
+ Ybp 1
- Ybp 1
H2O2
0 0.5 1 2 3
0 0.5 1 2 3 min
MW
170
110
80
70
HMW
Orp1-Yap 1
Orp1-Yap 1
Yap 1red
Ybp 1
Yap 1ox

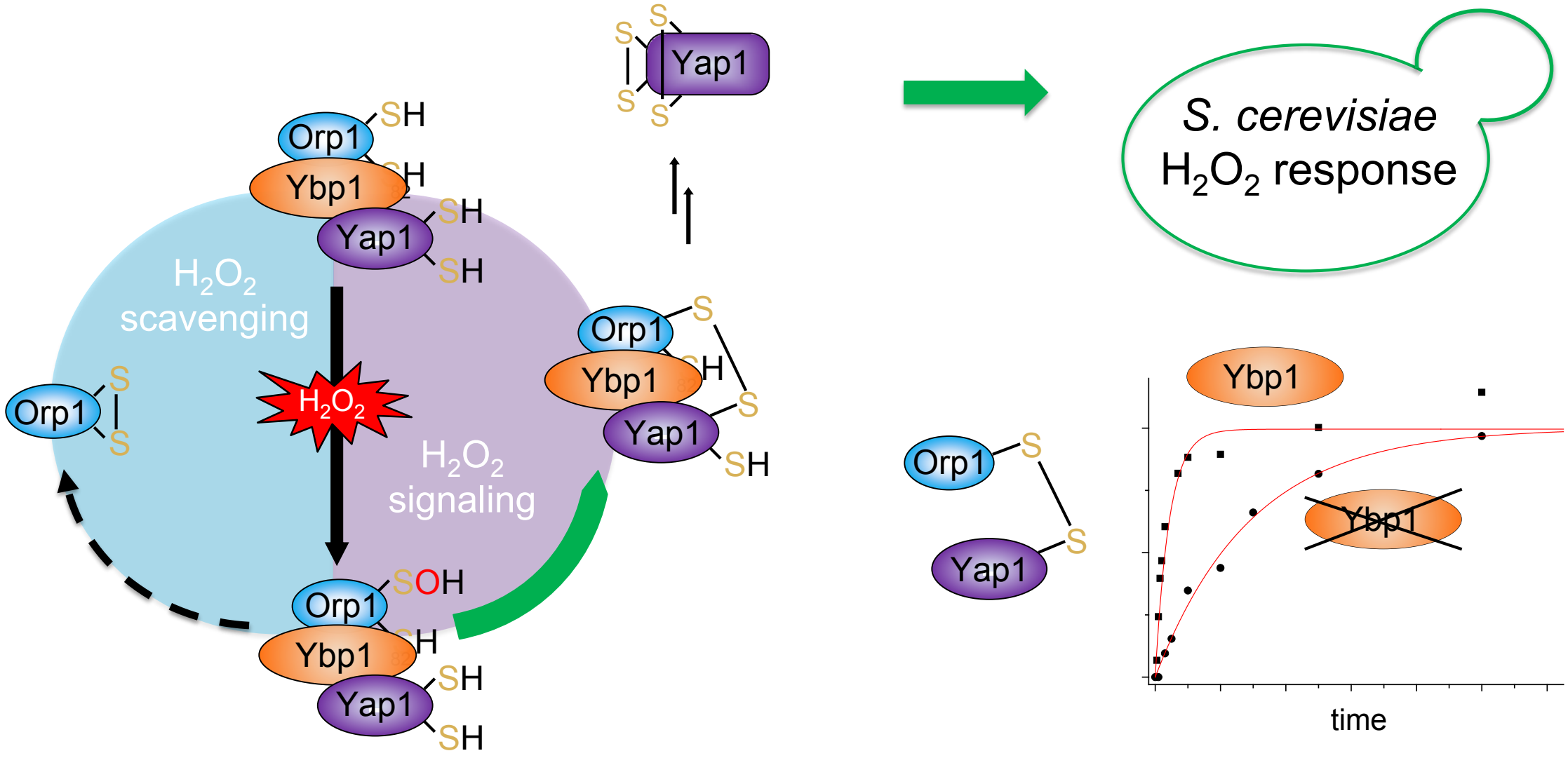
Yap1
Orp1
Ybp1
Yap1
H_2O_2 scavenging
H_2O_2
H_2O_2 signaling
Orp1
Ybp1
Yap1
Orp1
Ybp1
Yap1
S. cerevisiae
H_2O_2 response
Orp1
Yap1
Ybp1
Ybp1
time